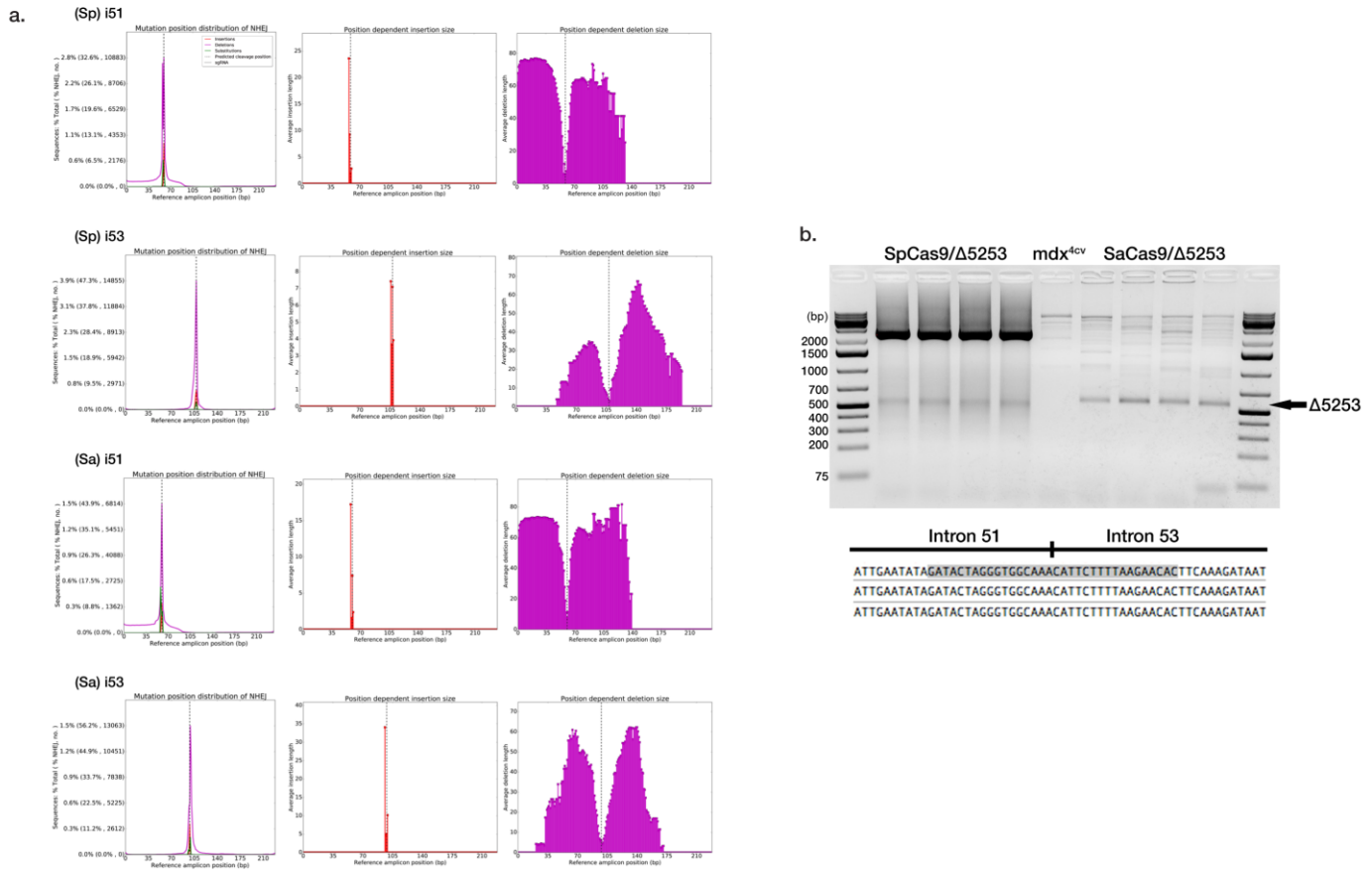
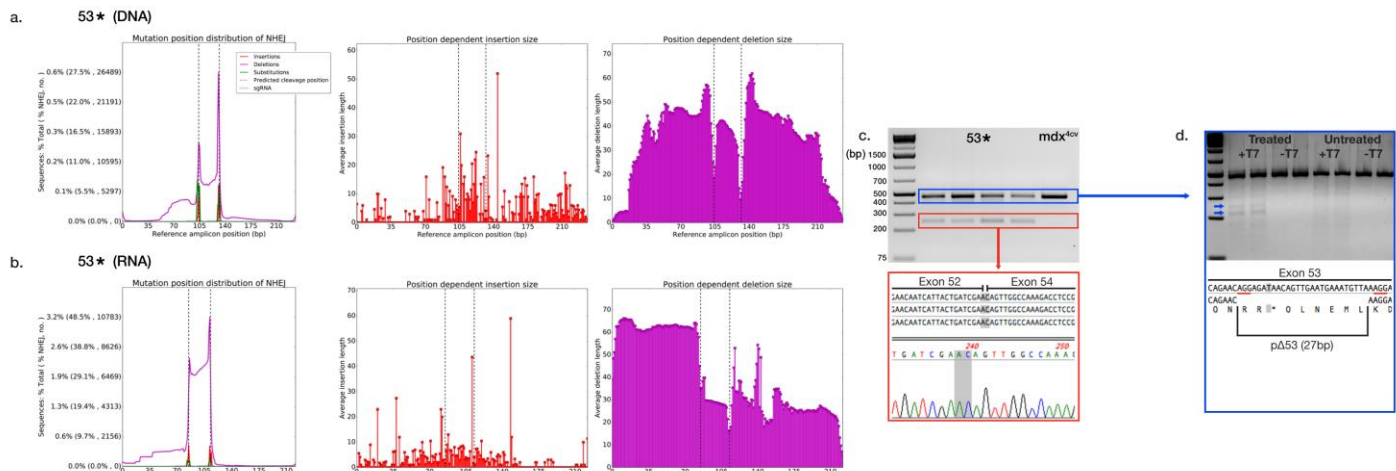


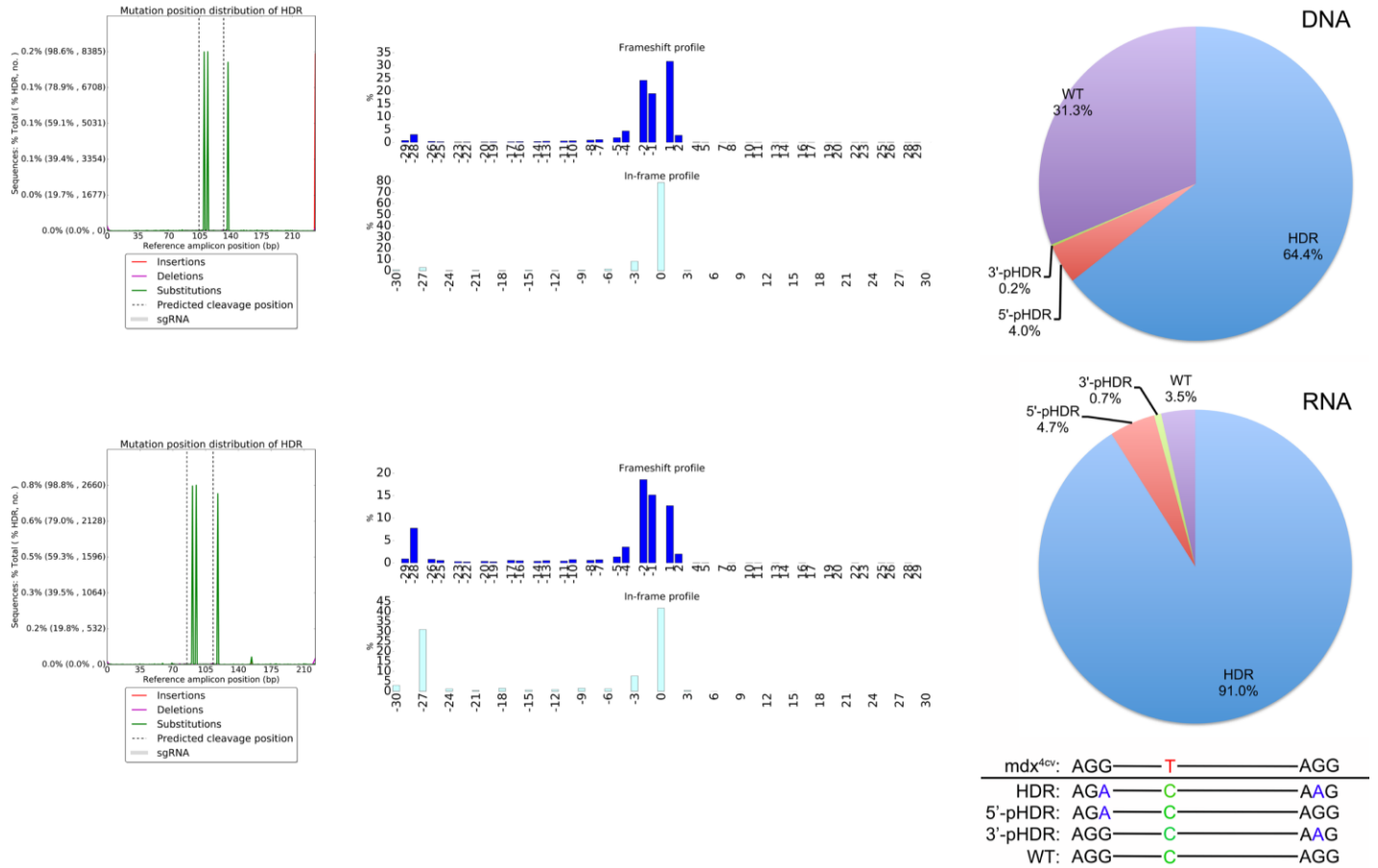
Supplementary Figure 1: *In vitro* validation of targeting constructs. *In vitro* editing efficiency at target sites within exon 53 (53*, strategy 2) as well as within introns 51 and 53 (Δ5253, strategy 1) was determined via the T7 endonuclease 1 assay following nuclease- and targeting construct electroporation into primary dermal fibroblasts isolated from *mdx^{4cv}* mice. For strategy 2, the two target sites within exon 53 were analyzed together due to their close proximity to each other. Efficiency estimated via densitometry measurements of unique cleavage bands.



Supplementary Figure 2: Analyses of gene editing efficiency for strategy 1. Graphs generated by the CRISPResso software pipeline during genomic deep sequencing analysis of PCR amplicons generated across the target sites within intron 51 (i51) and intron 53 (i53) for strategy 1 ($\Delta 5253$). (a) Shown are the percentages of insertions, deletions and substitutions, resulting from NHEJ events, for each nucleotide position across the PCR amplicon (left panels). The y-axis represents % total genomes or (% genomes, number of genomes exhibiting NHEJ). Also shown is the average insertion size (center panels) and average deletion size (right panels) at each nucleotide position across the PCR amplicons. Dotted lines represent predicted Cas9 cleavage sites. (b) PCR across the ~45 kb region targeted for deletion on DNA isolated from TAs treated with strategy 1 ($\Delta 5253$, n=4) shows the presence of a unique product (arrow) that by subsequent cloning and sequencing was determined to correlate to a merging of introns 51 and 53 as predicted.

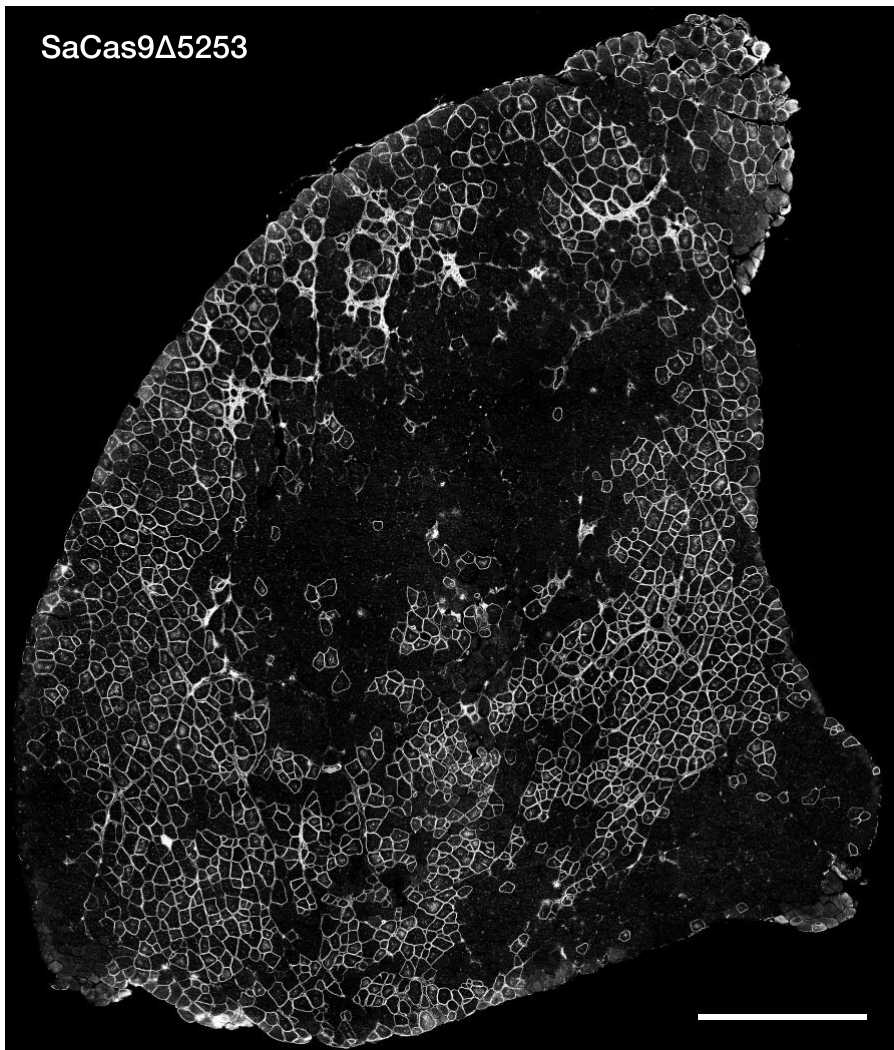


Supplementary Figure 3: Analyses of gene editing efficiency for strategy 2. Graphs generated during CRISPResso analysis for strategy 2 (53) during deep sequencing analysis of pooled PCR (**a**, n=5), and RT-PCR (**b**, n=4) amplicons generated across the target sites within exon 53 for strategy 2 (53*). Shows are the percentages of insertions, deletions and substitutions, resulting from NHEJ events, for each nucleotide position across the amplicons (left panels). The y-axis represents % total genomes or (% genomes, number of genomes exhibiting NHEJ). Also shown are the average insertion size (center panels) and average deletion size (right panels) at each nucleotide position across the amplicons. Dotted lines represent predicted Cas9 cleavage sites. (**c**) RT-PCR of target region transcripts isolated from TAs treated with strategy 2 (53*, n=4) shows the presence of a shorter product (red box) making up approximately 20% of total transcripts (based on image densitometry). Subsequent cloning and sequencing revealed that this product corresponded to out-of-frame transcripts lacking the sequences encoded on exon 53. (**d**) T7 endonuclease 1 digestion of the predominant top RT-PCR product from muscles treated with strategy 2 (blue box in **c**) indicates the presence of unique transcripts, making up approximately 11.2% of the analyzed RT-PCR product based on image densitometry (Top, blue arrows). Also shown is the DNA sequence of one clone of the RT-PCR products, revealing an in-frame transcript where the nonsense mutation was removed by a 27 bp in-frame deletion (bottom).

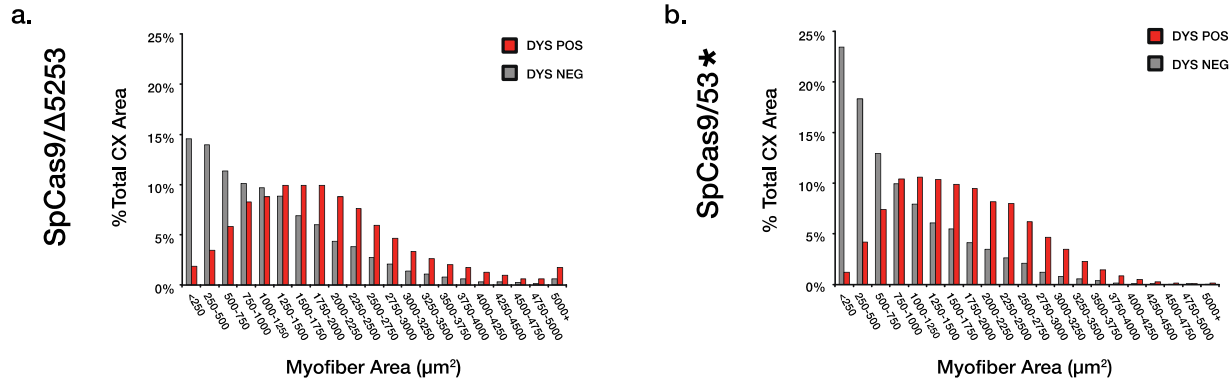


Supplementary Figure 4: HDR and reading frame analyses for strategy 2. Graphical representation of HDR detection, reading frame analysis and distribution of HDR genotypes for exon 53 based on deep sequencing of pooled PCR amplicons generated from genomic DNA (**top, n=5**) or transcripts (cDNA) (**bottom, n=4**) isolated from muscles treated with strategy 2 (53*). (**Left panels**) Show the percentages of HDR-derived nucleotide substitutions for each position across the amplicons, as generated by the CRISPResso software pipeline. The y-axis represents % total genomes or (% genomes, number of genomes exhibiting HDR). The graph demonstrates nucleotide substitutions at sites corresponding to the two silent PAM site mutations (G to A) and at the site of the *mdx^{4cv}* C to T point mutation. Dotted lines represent predicted Cas9 cleavage sites. (**Middle panels**) Show the size distributions of frameshift and in-frame reads, as generated by the CRISPResso (middle panels). The y-axis represents % of frameshift or in-frame reads while the x-axis represent the size of the corresponding deletions, insertions and substitutions. (**Right panels**) Show the genotypes and corresponding frequencies of HDR events resulting in the substitution of the *mdx^{4cv}* T mutation (red) to the WT C nucleotide (green). Genotypes resulting from successful HDR consisted of substitutions for: the complete HDR template (HDR), a partial HDR template from the 5'- or 3' ends (5'/3'-pHDR) and substitution of T to C without the PAM site mutations (WT). The silent PAM site mutations are depicted in blue. Of note, WT genotypes may in fact contain a large proportion of background reads, based on the level of reads observed with random single nucleotide substitutions and in untreated control RNA samples (supplemental tables 2-3). The remaining HDR reads containing 2 or 3 defined HDR specific nucleotide substitutions appear highly specific as these reads exhibit close to zero prevalence in untreated RNA samples (supplementary table 3).

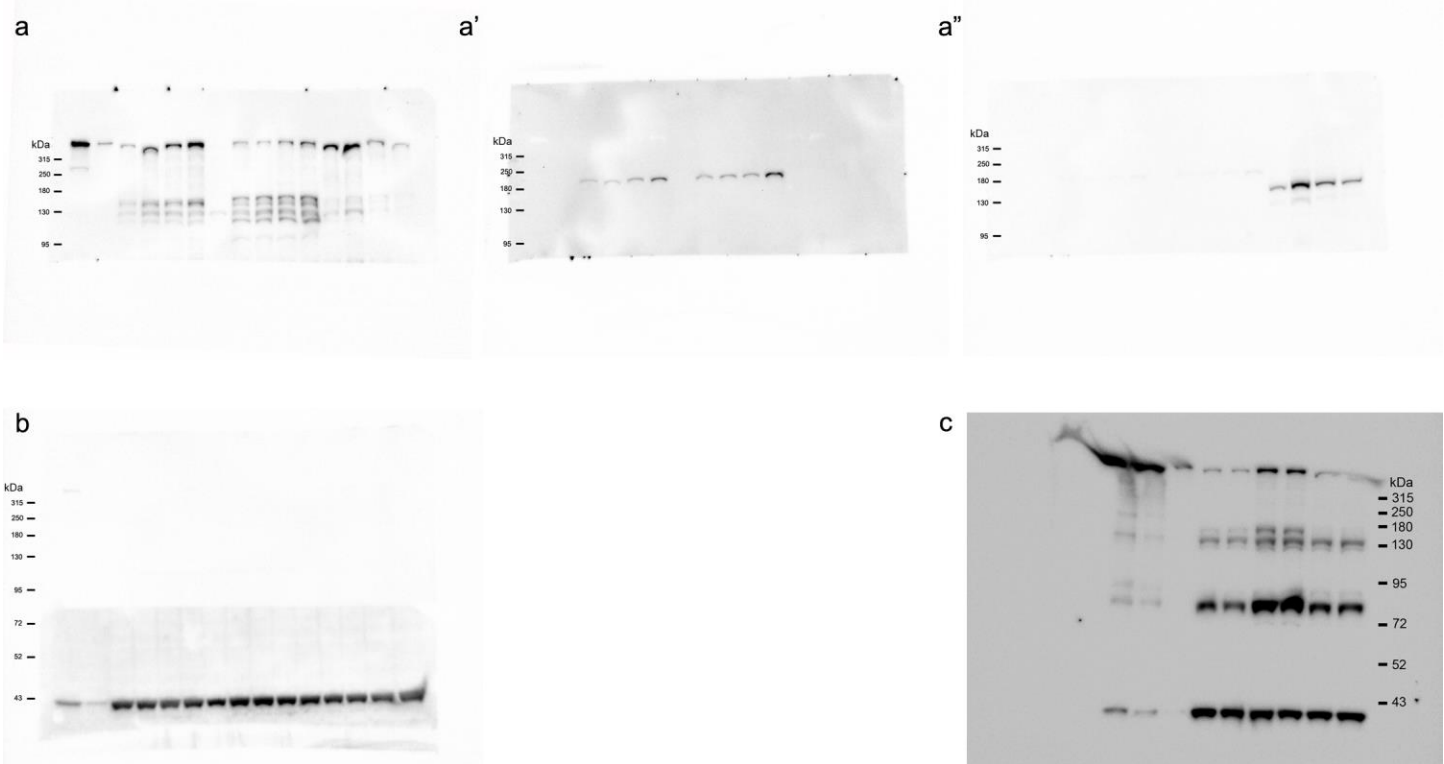
SaCas9Δ5253



Supplementary Figure 5: IF analysis for single vector approach in strategy 1. Dystrophin expression (white) detected in treated TA muscles injected with the single AAV6/SaCas9Δ5253 vector (n=4), analyzed at 4 weeks post-transduction (scale bar = 1000 μm).



Supplementary Figure 6: Size distribution analysis for individual myofibers in treated TA muscles. Cross-sectional area of individual, dystrophin- positive and negative myofibers from transduced TA muscles (n=4 ($\Delta 5253$), n=5 (53*) muscles; >25,000 myofibers traced per treatment). Transduced myofibers expressing dystrophin were larger than degenerating dystrophin-negative myofibers following IM injection (a and b), with a 5- and 10-fold reduction in myofibers under $250 \mu\text{m}^2$, respectively.



Supplementary Figure 7: Uncropped western blots used in figures 3 and 5. **a-b)** Western blot of TA lysates in figure 3 w as cut in half and the top part w as stained w ith antibodies against dystrophin (**a**), SpCas9 (**a'**) or HA-SaCas9 (**a''**). This blot w as stripped betwe en each subsequent antibody staining and some residual signal from the SpCas9 staining can be seen in the HA-SaCas9 blot in **a''**. The bottom part of the blot w as stained for GAPDH (**b**). **c)** Western blot of cardiac lysates following systemic gene editing w as cut in half and stained w ith antibodies against dystrophin (top half, >72 kDa), or GAPDH (bottom half, <72 kDa).

ON Target:	sgRNA sequence (5'-3')	Chromosome	Position	Total reads	NHEJ	HDR	NHEJ/HDR (mixed)	Editing efficiency (%)	HDR (%)
DNA:									
(Sp) i51	GATACTAGGGTGGCAAATAG	X	84530675-84530694	387126	33348	0	0	8.61	0.00
(Sp) i53	GTTGTTCTAAAGAATGGTG	X	84576353-84576372	383505	31411	0	0	8.19	0.00
(Sa) i51	GATACTAGGGTGGCAAATAGA	X	84530675-84530695	448016	15533	0	0	3.47	0.00
(Sa) i53	GAGATAAAATCCTGCTTATCAC	X	84576316-84576337	870140	23263	0	0	2.67	0.00
(Sp) 53*-5' (combined w. 3')	(G)TCAAGAACAGCTGCAGAAC	X	84575591-84575609	4681379	96177	8507	1421	2.27	0.18
(Sp) 53*-3' (combined w. 5')	(G)CAGTTGAATGAAATGTTAA	X	84575619-84595637						
RNA:									
(Sp) 53* (Treated, combined)				336095	22245	2692	5944	9.19	0.80
(Sp) 53* (Control, combined)				486042	1292	0	26	0.27	0.00

Supplementary Table 1: Deep sequencing quantification of editing efficiency and HDR events using CRISPResso. Efficient targeting was observed at all target sites for the different approaches. For NHEJ events, the majority of edited reads corresponded to deletions followed by insertions and substitutions (supplementary Fig. 1 & 2). For strategy 2, on-target deep sequencing was performed on DNA and cDNA generated from RNA isolated from treated muscles. Comparing DNA to RNA revealed an increase in both editing efficiency and prevalence of reads corresponding to successful HDR events at the transcript level, likely due to protection of functional edited transcripts against nonsense mediated decay. The sequence used to detect HDR events using CRISPResso included the WT cytosine at the site of the point mutation and both PAM site mutations. HDR quantification does not include mixed NHEJ/HDR events.

DNA HDR genotypes: Query sequence	Genotype	Reads detected (treated)	% of unaltered reads (Treated)	Reading frame
CAAGAA CAGCTGCGAACAGGAGATAACAGTTGAATGAAATGTAAAGATTCAACACAA	mdx	2532317	100	Unaltered in frame
CAAGAA CAGCTGCGAACAGGAGAACACAGTTGAATGAAATGTAAAGATTCAACACAA	WT	2294	0.091	In frame
CAAGAA CAGCTGCGAACAGAAGACAAAGTTGAATGAAATGTAAAGATTCAACACAA	HDR	4714	0.186	In frame
CAAGAA CAGCTGCGAACAGAAGACAAAGTTGAATGAAATGTAAAGATTCAACACAA	5'-pHDR	295	0.012	In frame
CAAGAA CAGCTGCGAACAGGAGAACACAGTTGAATGAAATGTAAAGATTCAACACAA	3'-pHDR	17	0.001	In frame
<i>Selected single substitutions (background)</i>				
CAAGAA CAGCTGCGAACAGGAGAACACAGTTGAATGAAATGTAAAGATTCAACACAA	N/A	852	0.034	In frame
CAAGAA CAGCTGCGAACAGGAGAACACAGTTGAATGAAATGTAAAGATTCAACACAA	N/A	325	0.013	In frame
CAAGAA CAGCTGCGAACAGCAGATAACAGTTGAATGAAATGTAAAGATTCAACACAA	N/A	211	0.008	In frame
CAAGAA CAGCTGCGAACAGTAGATAACAGTTGAATGAAATGTAAAGATTCAACACAA	N/A	766	0.030	In frame
CAAGAA CAGCTGCGAACAGGAGATAACAGTTGAATGAAATGTAAAGATTCAACACAA	N/A	119	0.005	In frame
CAAGAA CAGCTGCGAACAGGAGATAACAGTTGAATGAAATGTAAAGATTCAACACAA	N/A	743	0.029	In frame
DNA pΔ53 (w/o STOP) genotypes: Query sequence	Deletion size (bp)	Reads detected (Treated)	% of unaltered reads (Treated)	Reading frame
CAAGAA CAGCTGCGAACAGGAGATAACAGTTGAATGAAATGTAAAGATTCAACACAA	0	2532317	100	Unaltered in frame
CAAGAA CAGCTGCGAACAGGAGAACACAGTTGAATGAAATGTAAAGATTCAACACAA	3	1	0.000	In frame
CAAGAA CAGCTGCGAACAGGAGAACACAGTTGAATGAAATGTAAAGATTCAACACAA	6	0	0.000	In frame
CAAGAA CAGCTGCGAACACCAGTTGAATGAAATGTAAAGATTCAACACAA	9	0	0.000	In frame
CAAGAA CAGCTGCGAACAGGAGAACACAGTTGAATGAAATGTAAAGATTCAACACAA	12	1	0.000	In frame
CAAGAA CAGCTGCGAACAGGAGAACACAGTTGAATGAAATGTAAAGATTCAACACAA	15	0	0.000	In frame
CAAGAA CAGCTGCGAACAGGAGAACACAGTTGAATGAAATGTAAAGATTCAACACAA	15	0	0.000	In frame
CAAGAA CAGCTGCGAACAGGAGAACACAGTTGAATGAAATGTAAAGATTCAACACAA	18	0	0.000	In frame
CAAGAA CAGCTGCGAACAGGAGAACACAGTTGAATGAAATGTAAAGATTCAACACAA	18	44	0.002	In frame
CAAGAA CAGCTGCGAACACATGTAAAGATTCAACACAA	21	0	0.000	In frame
CAAGAA CAGCTGCGAACAGGTTAAAGATTCAACACAA	21	2	0.000	In frame
CAAGAA CAGCTGCGAACATGTAAAGATTCAACACAA	24	2	0.000	In frame
CAAGAA CAGCTGCGAACACTAAAGATTCAACACAA	24	50	0.002	In frame
CAAGAA CAGCTGCGAACACAAGATTCAACACAA	27	1	0.000	In frame
CAAGAA CAGCTGCGAACAGGATTCAACACAA	27	901	0.036	In frame
CAAGAA CAGCTGCGAACAGGATTCAACACAA	30	14	0.001	In frame
CAAGAA CAGCTGCGAACAGGATTCAACACAA	30	55	0.002	In frame
CAAGAA CAGCTGCGAACAGGATTCAACACAA	33	14	0.001	In frame
CAAGAA CAGCTGCGAACAGGATTCAACACAA	33	1	0.000	In frame
CAAGAA CAGCTGCGAACAGGATTCAACACAA	36	0	0.000	In frame
CAAGAA CAGCTGCGAACACAA	36	4	0.000	In frame
<i>Predicted cleavage site deletion product (PAM -3 bp)</i>				
CAGCTGCAGTAAAGATTCAACAA	28	1243	0.049	Out of frame
Exon 53, PAM, mdx (T) mutation, Substitutions				

Supplementary Table 2: Manual genotype analysis of genomic DNA for strategy 2. Manual analysis of deep sequencing reads within the Fastq file for on-target PCR amplicons generated from DNA isolated from muscles treated according to strategy 2 (53*). (**Top**) Prevalence of deep sequencing reads corresponding to different HDR derived genotypes and random single nucleotide substitutions (proposed background) at sites of particular interest. (**Bottom**) Prevalence of selected sequences corresponding to partial in-frame deletions (pΔ53) resulting in the removal of the *mdx*^{4cv} stop codon. The 28 bp out-of-frame deletion sequence predicted to be most prevalent, resulting from DNA cleavage at the prototypical PAM -3 nucleotide position, is indeed found most frequently among the deletions followed by a 27 bp in-frame deletion sequence.

RNA HDR genotypes: Query sequence	Genotype	Reads detected		% of unaltered reads		Reading frame
		mdx control	Treated	mdx control	Treated	
ATCGA <ins>TTGAAAGAACATTCACTGGATGAGGTCAAGAACAGCTGAGAACAGGAGATAACAGTGAATGAAATGTTAAAGGATT</ins> C	mdx	242375	154693	100	100	Unaltered in frame
ATCGA <ins>TTGAAAGAACATTCACTGGATGAGGTCAAGAACAGCTGAGAACAGGAGACAACAGTGAATGAAATGTTAAAGGATT</ins> C	WT	104	45	0.043	0.029	In frame
ATCGA <ins>TTGAAAGAACATTCACTGGATGAGGTCAAGAACAGCTGAGAACAGGAGACAACAGTGAATGAAATGTTAAAGGATT</ins> C	HDR	0	1130	0.000	0.730	In frame
ATCGA <ins>TTGAAAGAACATTCACTGGATGAGGTCAAGAACAGCTGAGAACAGGAGACAACAGTGAATGAAATGTTAAAGGATT</ins> C	5'-pHDR	0	61	0.000	0.039	In frame
ATCGA <ins>TTGAAAGAACATTCACTGGATGAGGTCAAGAACAGCTGAGAACAGGAGACAACAGTGAATGAAATGTTAAAGGATT</ins> C	3'-pHDR	0	7	0.000	0.005	In frame
<i>Selected single substitutions (background)</i>						
ATCGA <ins>TTGAAAGAACATTCACTGGATGAGGTCAAGAACAGCTGAGAACAGGAGAGAACAGTGAATGAAATGTTAAAGGATT</ins> C	N/A	24	17	0.010	0.011	In frame
ATCGA <ins>TTGAAAGAACATTCACTGGATGAGGTCAAGAACAGCTGAGAACAGGAGAGAACAGTGAATGAAATGTTAAAGGATT</ins> C	N/A	20	5	0.008	0.003	In frame
ATCGA <ins>TTGAAAGAACATTCACTGGATGAGGTCAAGAACAGCTGAGAACAGCAGATAACAGTGAATGAAATGTTAAAGGATT</ins> C	N/A	21	4	0.009	0.003	In frame
ATCGA <ins>TTGAAAGAACATTCACTGGATGAGGTCAAGAACAGCTGAGAACAGCAGATAACAGTGAATGAAATGTTAAAGGATT</ins> C	N/A	83	49	0.034	0.032	In frame
ATCGA <ins>TTGAAAGAACATTCACTGGATGAGGTCAAGAACAGCTGAGAACAGGAGATAACAGTGAATGAAATGTTAAACGATT</ins> C	N/A	17	3	0.007	0.002	In frame
ATCGA <ins>TTGAAAGAACATTCACTGGATGAGGTCAAGAACAGCTGAGAACAGGAGATAACAGTGAATGAAATGTTAAATGATT</ins> C	N/A	93	51	0.038	0.033	In frame
RNA pΔ53 (w/o STOP) genotypes: Query sequence	Deletion size (bp)	Reads detected		% of unaltered reads		Reading frame
		mdx control	Treated	mdx control	Treated	
ATCGA <ins>TTGAAAGAACATTCACTGGATGAGGTCAAGAACAGCTGAGAACAGGAGA(TAA)CAGTGAATGAAATGTTAAAGGATT</ins> C	0	242375	154693	100	100	Unaltered in frame
ATCGA <ins>TTGAAAGAACATTCACTGGATGAGGTCAAGAACAGCTGAGAACAGGAGAGAACAGTGAATGAAATGTTAAAGGATT</ins> C	3	0	0	0.000	0.000	In frame
ATCGA <ins>TTGAAAGAACATTCACTGGATGAGGTCAAGAACAGCTGAGAACAGCAGATAACAGTGAATGAAATGTTAAAGGATT</ins> C	6	0	0	0.000	0.000	In frame
ATCGA <ins>TTGAAAGAACATTCACTGGATGAGGTCAAGAACAGCTGAGAACACCAGTGAATGAAATGTTAAAGGATT</ins> C	9	0	0	0.000	0.000	In frame
ATCGA <ins>TTGAAAGAACATTCACTGGATGAGGTCAAGAACAGCTGAGAACAGCTGAGACAGTGAATGAAATGTTAAAGGATT</ins> C	12	0	0	0.000	0.000	In frame
ATCGA <ins>TTGAAAGAACATTCACTGGATGAGGTCAAGAACAGCTGAGAACAGGAAAATGTTAAAGGATT</ins> C	15	0	0	0.000	0.000	In frame
ATCGA <ins>TTGAAAGAACATTCACTGGATGAGGTCAAGAACAGCTGAGAACAGGAGAAATGTTAAAGGATT</ins> C	15	0	0	0.000	0.000	In frame
ATCGA <ins>TTGAAAGAACATTCACTGGATGAGGTCAAGAACAGCTGAGAACAGGAGATAACAGTGAATGTTAAAGGATT</ins> C	18	0	0	0.000	0.000	In frame
ATCGA <ins>TTGAAAGAACATTCACTGGATGAGGTCAAGAACAGCTGAGAACAGGAGATAACAGTGAATGTTAAAGGATT</ins> C	18	0	87	0.000	0.056	In frame
ATCGA <ins>TTGAAAGAACATTCACTGGATGAGGTCAAGAACAGCTGAGAACAGCTGAGACATGTTAAAGGATT</ins> C	21	0	0	0.000	0.000	In frame
ATCGA <ins>TTGAAAGAACATTCACTGGATGAGGTCAAGAACAGCTGAGAACAGCTGAGACAGGTTAAAGGATT</ins> C	21	0	2	0.000	0.001	In frame
ATCGA <ins>TTGAAAGAACATTCACTGGATGAGGTCAAGAACAGCTGAGAACAGCTGAGATGTTAAAGGATT</ins> C	24	0	7	0.000	0.005	In frame
ATCGA <ins>TTGAAAGAACATTCACTGGATGAGGTCAAGAACAGCTGAGAACACTAAAGGATT</ins> C	24	0	42	0.000	0.027	In frame
ATCGA <ins>TTGAAAGAACATTCACTGGATGAGGTCAAGAACAGCTGAGAACAGGATT</ins> C	27	0	6	0.000	0.004	In frame
ATCGA <ins>TTGAAAGAACATTCACTGGATGAGGTCAAGAACAGCTGAGATGTTAAAGGATT</ins> C	27	2	1253	0.001	0.810	In frame
ATCGA <ins>TTGAAAGAACATTCACTGGATGAGGTCAAGAACAGCTGAGCTAAAGGATT</ins> C	30	0	35	0.000	0.023	In frame
ATCGA <ins>TTGAAAGAACATTCACTGGATGAGGTCAAGAACAGCTGAGAGGATT</ins> C	30	0	64	0.000	0.041	In frame
ATCGA <ins>TTGAAAGAACATTCACTGGATGAGGTCAAGAACAGCTGAGAGGATT</ins> C	33	0	19	0.000	0.012	In frame
ATCGA <ins>TTGAAAGAACATTCACTGGATGAGGTCAAGAACAGCTGAGAGGATT</ins> C	33	0	0	0.000	0.000	In frame
ATCGA <ins>TTGAAAGAACATTCACTGGATGAGGTCAAGAACAGGATT</ins> C	36	0	2	0.000	0.001	In frame
ATCGA <ins>TTGAAAGAACATTCACTGGATGAGGTCAAGAACAGCTGAGGATT</ins> C	36	0	2	0.000	0.001	In frame
<i>Predicted cleavage site deletion product (PAM -3 bp)</i>						
ATCGA <ins>TTGAAAGAACATTCACTGGATGAGGTCAAGAACAGCTGAGAAAGGATT</ins> C	28	0	582	0.000	0.376	Out of frame

Exon 52, Exon 53, PAM, mdx (T) mutation, Substitutions

Supplementary Table 3: Manual genotype analysis of transcripts for strategy 2. Manual analysis of deep sequencing reads within the Fastq files for on-target RT-PCR amplicons generated from RNA isolated from untreated- (mdx control) and treated muscles according to strategy 2 (53*). (**Top**) Prevalence of deep sequencing reads corresponding to different HDR derived genotypes and random single nucleotide substitutions (proposed background) at sites of particular interest. The presence of reads with single nucleotide substitutions within the untreated sample indicates the level of natural variation and/or sequencing errors. Interestingly, inclusion of 2 or more substitutions at defined positions in the query virtually eliminates detection in untreated controls. (**Bottom**) Prevalence of selected sequences corresponding to partial in-frame deletions (pΔ53) resulting in the removal of the *mdx*^{4cv} stop codon. The sequence generated following removal of 27 bp between the two target sites appears to be the most prevalent. The 28 bp out-of-frame deletion sequence, predicted to be most prevalent following cleavage at the prototypical PAM -3 nucleotide position, appears less prominent at the transcript level than at the DNA level (as shown in supplementary table 2).

OFF Target:	sgRNA sequence (5'-3')	Chromosome	Position	Total reads	Modified Reads	Editing efficiency (%)
(Sp) sgRNAi51	GATACTAGGGTGGCAAATAG					
OT#1	GATACTAG T GTGG C TATAG	3	141701844-141701863	552579	1068	0.19
OT#2	GATA C ATGGTGGCAAAT C G	7	130395430-130395449	402732	1146	0.28
OT#3	GATACTAGGGTGG G GAATAA	18	39792989-39793008	517898	2297	0.44
(Sp) sgRNAi53	GTGTTCTTAAAAGAAATGGTG					
OT#1	T TTTCTTAAAAGAAATGG A	17	5033249-5033268	287696	1689	0.59
OT#2	T TGATCTTA G AGAAATGGTG	X	164639812-164639831	48548	178	0.37
OT#3	GT T TCTTGAAA A ATGGTG	17	86877921-86877940	406556	2047	0.50
OT#4	C TGTTCTTAAAAG G TGGTG	4	85991645-85991664	435323	2702	0.62
OT#5	G AGTTCTTC A AGAAAT G TG	2	64505959-64505978	485078	1653	0.34
(Sp) sgRNA-5'	(G)TCAAGAACAGCTGCAGAAC					
OT#1	TCT AG GGCAGCTGCAGAAC	14	11161529-11161547	757561	2729	0.36
OT#2	TC A TT C ACAGCTGCAGAAC	2	30938892-30938910	347367	949	0.27
OT#3	C AAGAACAGCTGCAG A AC	11	58117430-58117448	421793	873	0.21
OT#4	TCAAGAACAGCTGCAG C AG	15	3176773-3176791	370386	2396	0.65
OT#5	TCAAGAACAGCTGC A T C AC	18	27855793-27855811	459555	1846	0.40
(Sp) sgRNA-3'	(G)CAGTTGAATGAAATGTTAA					
OT#1	CAGTT A CATGAAATGTTAA	3	106429607-106429625	430282	1261	0.29
OT#2	C ATT T AATGAAATGTTAA	7	86738658-86738676	495137	1978	0.40
OT#3	A AGTTGAATGAAAT T TTAA	5	63409984-63410002	275293	1531	0.56
OT#4	CAGT G AATAAAATGTTAA	2	23248164-23248182	145528	1369	0.94

Supplementary Table 4: Genomic off-target analyses. Deep sequencing quantification of gene editing frequency at the top predicted potential off-target sites for each gRNA reveals low levels of sequence variation (nucleotide mismatches from the on-target sequence are highlighted in blue). The vast majority of edited reads detected at potential off-target sites correspond to single nucleotide substitutions. Few deletion- and insertion events are randomly distributed across the amplicons, indicating low levels of natural variation and/or sequencing errors.

5'-GTACCTTCTAATAAAATAATTGTTATTAGTGTAGACTAAAGTTGAATTATTTCTAACATGGCA
CCAATATTGTAGTTATTCAATGCAAGTAATTAAATAGAAAGTCAAATTGTCACCTGAAGAAATGATTTGTTAATTATTTACCTAT
ATCACTCATAGCACCTGGATATATTAAATGAGAAATATACATGTCAATGACGTTAGATTCTAAATTCCACTGTCTCTTGAGTA
ATAATTACTGTTCTTATTCTTATTCCAGTTGAAGAATTCAAGATTCAAGCTAGTGGGATGAGGTTCAAGAACAG CTGCAGAACAG AA
GACAACAGTTGAATGAAATGTTAAAAGATTCAACACAATGGCTGGAAGCTAAGGAAGAACGCCAACAGGTCAAGCAGGTCAG
AGGCAAGCTGACTCATGGAAGAAGGTCCCTCACACAGTAGATGCAATCCAAAAGAACATCACAGAAACCAAGGTTAGTGTCAAGC
ATATCTTAAAAAAATTTGTATAGCAAATGAAAGCATGCCATAAATTAAATGTTTCTTAGTG AAAATTACATTTAGGAA
GTGAAAAGTGGATTCTGCTGTTTGATTGGTTGGTTGGTTGGCTGGCTGGTGGCTGGTTGGCTGGTTGGCTGGTTGGCTGGTT
GGTTGGTTGGTTGGTTGAGACAAAATCTAAACTCAAGACTACAGATGAGTGCCACTACATCTACATGATTAAAAT
TTTGAGACACAGTATAGGTTATAGGAAAATG-3'

Supplementary Table 5: Sequence of the HDR fragment used in the AAV vectors shown in Figure 1c. The silent PAM site mutations that were introduced to prevent vector cleavage by Cas9 (G to A) are marked in blue. The wild type nucleotide (C) used for replacement of the *mdx*^{4cv} mutation (T) is marked in green.

SpCas9 subcloning			
Forward	ATGGCCCCAAGAAGAACGCG	Reverse	CTTACTTTCTTTTGCCCT
U6-(Sp)sgRNA cassette subcloning			
Forward	TCAGACCCACCTCCAAAC	Reverse	AATTCAAAAAGCACCGACTCG
U6-(Sa)sgRNA subcloning			
Forward	TCAGACCCACCTCCAAAC	Reverse	AATTCAAAAAGCACCGACTCG
sgRNA primers for Strategy A ($\Delta 5253$)			
SpCas9-intron 51 (Forward)	CACCGATACTAGGGTGGCAAATAG	SpCas9-intron 51 (Reverse)	AAACCTATTTGCCACCCTAGTATC
SpCas9- intron 53 (Forward)	CACCGTGTCTTAAAGAAATGGTG	SpCas9- intron 53 (Reverse)	AAACACCATTCTTTAAGAACAC
SaCas9- intron 51 (Forward)	CACCGATACTAGGGTGGCAAATAGA	SaCas9- intron 51 (Reverse)	AAACTCTATTTGCCACCCTAGTATC
SaCas9- intron 53 (Forward)	CACCGAGATAAAATCCCTGTTATCAC	SaCas9- intron 53 (Reverse)	AAACGTATAAGCAGGGATTATCTC
sgRNA primers for Strategy B (53^*), (preferred G inserted at 5' position)			
SpCas9-5' (Forward)	CACCGTCAAGAACAGCTGCAGAAC	SpCas9-5' (Reverse)	AAACGTTCTGCACTGTTCTGAC
SpCas9-3' (Forward)	CACCGCAGTTGAATGAAATGTAA	SpCas9-3' (Reverse)	AAACTTAACATTCACTCAACTGC
On-target PCR/RT-PCR primers			
PCR- $\Delta 5253$ (Forward)	CTCATACCAAAGCTGCTAG	PCR- $\Delta 5253$ (Reverse)	CCTTTAGCCTAGAGATGTC
PCR- 53^* (Forward)	GCTGAGGTAATAGAGCCAAG	PCR- 53^* (Reverse)	CTGTGATCTTCTTTGGATTGTC
RT-PCR_ $\Delta 5253$ (Forward)	GCCATCTCTTGTGTTGG	RT-PCR_ $\Delta 5253$ (Reverse)	TCCGAAGAAGTTCTAGTGC
RT-PCR_ 53^* (Forward)	CAGAGAGTGTGGGGTGA	RT-PCR_ 53^* (Reverse)	TCCGAAGAAGTTCTAGTGC
On-target deep sequencing primers			
DS_i51 (Forward)	CACACATTGCTTATGTTAAAGATTGG	DS_i51 (Reverse)	GCAACAAACACTTTAAACACTIGAG
DS_i53 (Forward)	ATGTCCTTGCCACCATGCTAA	DS_i53 (Reverse)	GCATCTTACTCTTCTAAGAAGAAATT
DS_53* (Forward)	TTTCCACTGTCCTCTTGAGTAA	DS_53* (Reverse)	CTACTGTGAGGACCTTCTTC
DS_RT53* (Forward)	CCAGCAATCAAGAAGCTAGAAC	DS_RT53* (Reverse)	GCATCTACTGTGAGGACCC
Off-target deep sequencing primers			
DS_i51OT#1 (Forward)	CTGTTGCTCATGGGCTCA	DS_i51OT#1 (Reverse)	ACAGTCTTCTAAACAGAAATGCT
DS_i51OT#2 (Forward)	CCAACGACTTTCTGAAACC	DS_i51OT#2 (Reverse)	GAAATGTCTTACCCAGTTTGC
DS_i51OT#3 (Forward)	GCCATCCTAAAGAACACCAAG	DS_i51OT#3 (Reverse)	TGGAGCACACATTAGCCATC
DS_i53OT#1 (Forward)	GATGGCTTTGAACTTGAGAGAG	DS_i53OT#1 (Reverse)	CTAACACACTCGGGAACTG
DS_i53OT#2 (Forward)	GAGTTGATTCTCTTCAATC	DS_i53OT#2 (Reverse)	TTCGTTCACCTACAGAAAG
DS_i53OT#3 (Forward)	AGCCTTACCGTTGGTACAG	DS_i53OT#3 (Reverse)	ATTCAATTACCTCATAGTTGCTGCT
DS_i53OT#4 (Forward)	CCTGTAACCAGAACAGCTTAG	DS_i53OT#4 (Reverse)	GTCACTGGTAGTTAATAGGGTACG
DS_i53OT#5 (Forward)	CACCTGTTGACGACAGAACAA	DS_i53OT#5 (Reverse)	AGTCAAATGACAAGACTATGGCTAC
DS_53*-5'OT#1 (Forward)	CGAGCCACAGTGAATTGATG	DS_53*-5'OT#1 (Reverse)	CGTCCATAGACAAGTGTCA
DS_53*-5'OT#2 (Forward)	GCTGCCTGGGAGGTTAGA	DS_53*-5'OT#2 (Reverse)	GGTTCACTTCTCAGTGGG
DS_53*-5'OT#3 (Forward)	CAATGGAGCAGAACAGCTG	DS_53*-5'OT#3 (Reverse)	GCACAGTCCACATCTCATTC
DS_53*-5'OT#4 (Forward)	GGCTTGGTTCACTTTCACTC	DS_53*-5'OT#4 (Reverse)	CTCAGTGGCAGTTGAATACCAAG
DS_53*-5'OT#5 (Forward)	GTCTCAGTCTCAGTGAACAGTG	DS_53*-5'OT#5 (Reverse)	GGCACAGCATGTAAGAGAT
DS_53*-3'OT#1 (Forward)	AGCAGGGTCGCTTGAG	DS_53*-3'OT#1 (Reverse)	GCTCACTTGACTTGAAGGC
DS_53*-3'OT#2 (Forward)	AGCATGGACAATGAGGAAC	DS_53*-3'OT#2 (Reverse)	CCTGGGTGTTTGCCTTCT
DS_53*-3'OT#3 (Forward)	TACAGGTGAGTTGACACACTCC	DS_53*-3'OT#3 (Reverse)	AGGATTTCAGCATCACTATCTAGC
DS_53*-3'OT#4 (Forward)	CCTTGGCATTCTGCCCTTCC	DS_53*-3'OT#4 (Reverse)	CATTCTGTGAGGTAACCCAG

Supplementary Table 6: List of primers. Primer pairs used for subcloning; SpCas9 from pSpCas9(BB)-2A-Puro (PX459) (Addgene plasmid# 48139) into the pAAV-CK8-SpCas9 nuclease vector, the U6-(Sp)sgRNA cassette from plasmid lentiCRISPRv1 (Addgene plasmid# 49535) into the pAAV- $\Delta 5253/53^*$ targeting vectors, an additional U6-(Sa)sgRNA cassette into the plasmid pX601-AAV-CMV::NLS-SaCas9-NLS-3xHA-bGHpA; U6::Bsal-sgRNA (Addgene plasmid# 61591), as well as sgRNA target sequences and primers used to amplify ON/OFF target sites for PCR, RT-PCR and deep sequencing (DS) analyses (sequences are shown in the 5'-3' orientation).